Conf-811108--23

NUMERICAL SIMULATION OF COMBINED NATURAL AND FORCED CONVECTION DURING THERMAL-HYDRAULIC TRANSIENTS

CONF-811108--23

DE83 009647

by

H. M. Domanus and W. T. Sha

ABSTRACT

The single-phase COMMIX (COMponent MIXing) computer code performs fully three-dimensional, transient, thermal-hydraulic analyses of liquid-sodium LMFBR components. It solves the conservation equations of mass, momentum, and energy as a boundary-value problem in space and as an initial-value problem in time. The concepts of volume porosity, surface permeability and distributed resistance, and heat source have been employed in quasi-continuum (rod-bundle) applications. Volume porosity is defined as the ratio of the volume occupied by the fluid to the total volume of the computational cell. Surface permeability is defined as the ratio of the flow area in a particular direction available for fluid to the total area in the same direction across a surface of the computational cell. Distributed resistance is the drag force due to the presence of rods and is distributed continuously throughout the computational cell. Distributed heat source is similarly defined as distributed resistance.

Results from three transient simulations involving forced and natural convection are presented: (1) a sodium-filled horizontal pipe initially of uniform temperature undergoing an inlet velocity rundown transient, as well as an inlet temperature transient; (2) a 19-pin LMFBR rod bundle undergoing a velocity transient; and, (3) a simulation of a water test of a 1/10-scale outlet plenum undergoing both velocity and temperature transients.

1. INTRODUCTION

It is important to know, or at least to have an indication of, flow and temperature fields within thermal-hydraulic components. This information is useful in evaluating operational performance as well as in assessing safety considerations. These tasks are best performed by a combined experimental and computer simulation effort. To aid these evaluations and assessments, new computational tools, the COMMIX computer codes, have been developed.

The COMMIX-1 (COMponent MIXing) computer code [1] performs three-dimensional, transient, single-phase, thermal-hydraulic analyses of liquid-sodium LMFBR components. It solves the conservation equations of mass, momentum, and energy as a boundary-value problem in space and as an initial-value problem in time for a wide range of geometric configurations and thermal-hydraulic operating conditions. The COMMIX computer code is being developed in a stage-wise manner, where new and/or improved models are progressively implemented into the code. The code is structured in modular fashion so that new models can readily be implemented.

The most recent version of the single-phase COMMIX code is called COMMIX-1A. This version contains many improvements to the original COMMIX-1

in both physical modeling and computing efficiency. The single-phase COMMIX code has been used to analyze both continuum and quasi-continuum applications [2-6].

In the course of developing COMMIX-1A, several simulations have been performed involving combined natural and forced convection. Here three different component simulations are discussed. In these simulations, forced convection is dominant initially, but as the transients proceed, buoyancy forces become increasingly important and can significantly alter the thermal hydraulics within these components.

2. POROUS-MEDIUM APPROACH

The porous-medium approach with volume porosity, surface permeability, distributed resistance, and distributed heat source (or sink) is employed in the COMMIX code for rod-bundle thermal-hydraulic analysis. It provides a greater range of applicability and an improved accuracy over subchannel analysis [7,8]. The volume porosity (γ_v) is defined as the ratio of the volume occupied by the fluid to the total volume of the computational cell. Surface permeabilities (γ_i) are similarly defined as the ratio of the surface area in the direction available to the fluid to the corresponding total surface area in the same direction. The distributed resistance force (R) in the momentum equation represents the sum of the drag force due to the presence of rods and the additional viscous force due to the difference between the fine structure and the cell-averaged velocity distribution in the computational cells. The distributed heat source (or sink) Q is normally taken as a local volumetric heat source. The concept of surface permeability is an additional feature added in the porous-medium formulation. This permits easy modeling of the anisotropic characteristics of a flow domain.

The porous medium can readily be reduced to a continuum by setting volume porosity and surface permeabilities to unity, and distributed resistance to zero. Thus, a single formulation is applicable to both quasi-continuum and continuum analyses.

2.1 Governing Equations

Conservation of Mass

$$\frac{D}{\gamma_v} = \frac{\partial \rho}{\partial t} + \frac{1}{\gamma_v} \nabla \cdot (\gamma_j \rho u)$$

Conservation of Momentum

$$\gamma_v \rho \frac{\partial u_i}{\partial t} + \gamma_v u_i \left(\frac{\partial \rho}{\partial t} - \frac{D}{\gamma_v} \right) + \frac{\partial}{\partial x_j} (\gamma_j \rho u_i u_j) =$$

$$- \gamma_i \frac{\partial P}{\partial x_i} + \frac{\partial}{\partial x_j} (\gamma_j \tau_{ji}) + \gamma_v \rho g_i + \gamma_v R_i$$

Conservation of Energy

$$\gamma_V \rho \frac{\partial h}{\partial t} + \gamma_V h \left(\frac{\partial \rho}{\partial t} - \frac{D}{\gamma_V} \right) + \frac{\partial}{\partial x_j} (\gamma_j \rho u_j h) =$$

$$\gamma_V \frac{dP}{dt} + \frac{\partial}{\partial x_j} \left(\gamma_j \kappa_{eff} \frac{\partial T}{\partial x_j} \right) + \gamma_V Q + \gamma_j \tau_{ji} \frac{\partial u_i}{\partial x_j}$$

Here ρ is the density, u_j are velocity vector components, g is the gravity vector, h is the enthalpy, P is the pressure, x_j is the coordinate direction, and t is the time. The terms γ_V, γ_j, R_i, and Q are the volume porosity, surface permeability, distributed resistance, and distributed heat source, respectively. The quantity D is the local mass residue of the continuity equation. In the above equations, a repeated index implies the sum of three terms.

3. LMFBR HORIZONTAL PIPE

The thermal hydraulics in a horizontal section of an LMFBR intermediate pipe loop during an LMFBR flow coastdown has been numerically simulated using the COMMIX-1A computer code. The purpose of the simulation is to investigate the thermal-buoyancy effects on temperature and velocity distributions in a pipe. Thermal-buoyancy-induced flows in piping can be important during both steady-state and transient operating conditions. Buoyancy can alter hydraulic resistance and create large, local temperature gradients.

A one-dimensional heat-transfer model has been used to simulate heat transfer between the pipe wall and liquid sodium.

3.1 Geometry

The pipe is horizontal and 21.336 m (70 ft) long. The inner diameter is 0.4318 m. The pipe wall thickness is 0.0127 m and is made of SS 316. Since the thermal-hydraulic conditions are symmetric with respect to the vertical centerline, half of the circular geometry is considered.

As shown in Fig. 1, the 21.336 m pipe is partitioned into 35 equal 0.6096 m lengths. The radial direction is partitioned into five 0.08636 m equal lengths. The azimuthal direction is partitioned into six equal 30° angles.

3.2 Operating Conditions

Initially, 358.8°C sodium enters the pipe with an average velocity of 6.364 m/s. Figure 2 shows the flow and temperature transient forcing functions at the inlet.

The following assumptions were used in this simulation:

1. The shape of the inlet velocity distribution is parabolic throughout the transient.

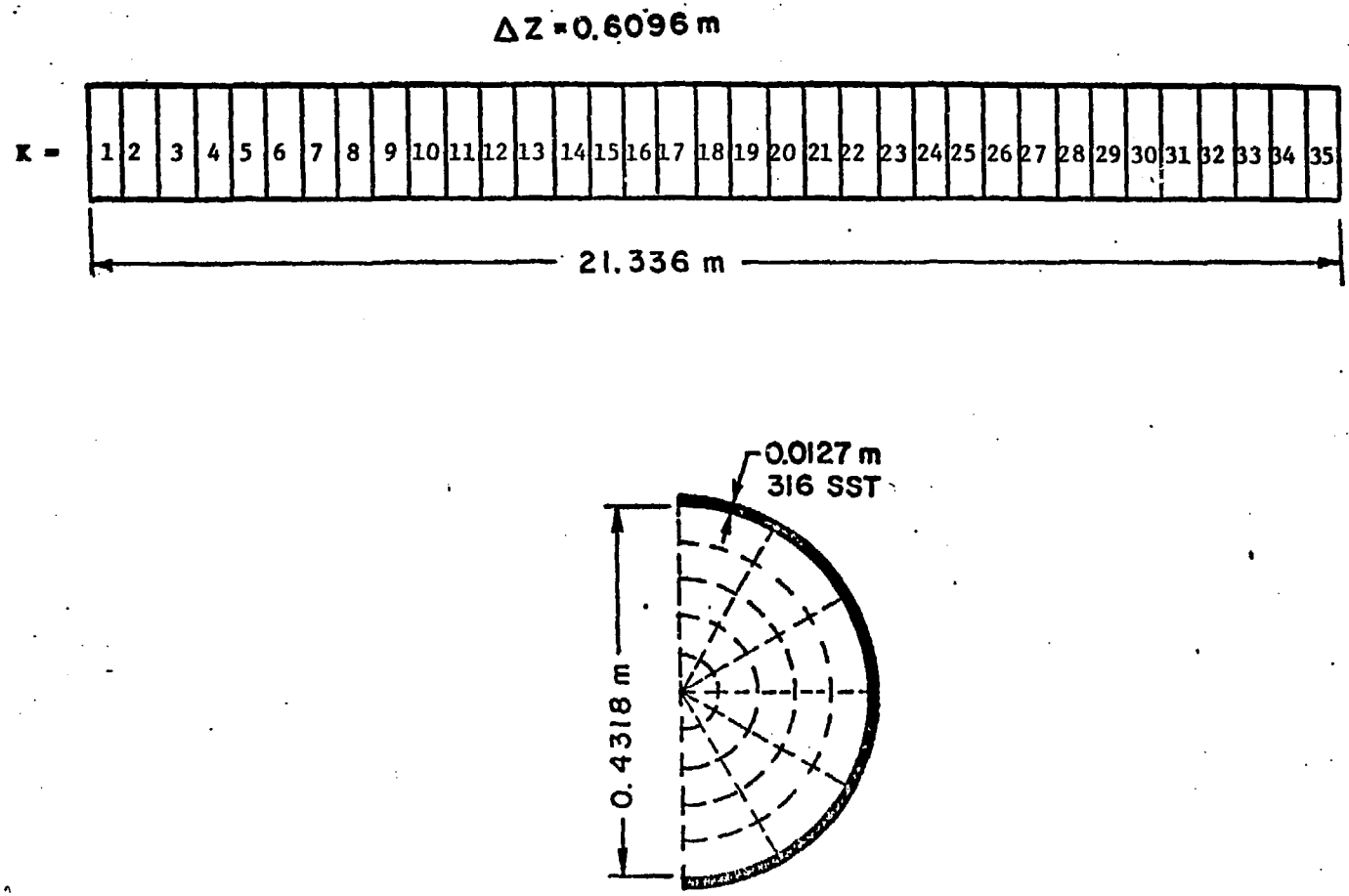

Fig. 1. Axial, Radial, and Azimuthal Partitioning Used for Pipe Simulation

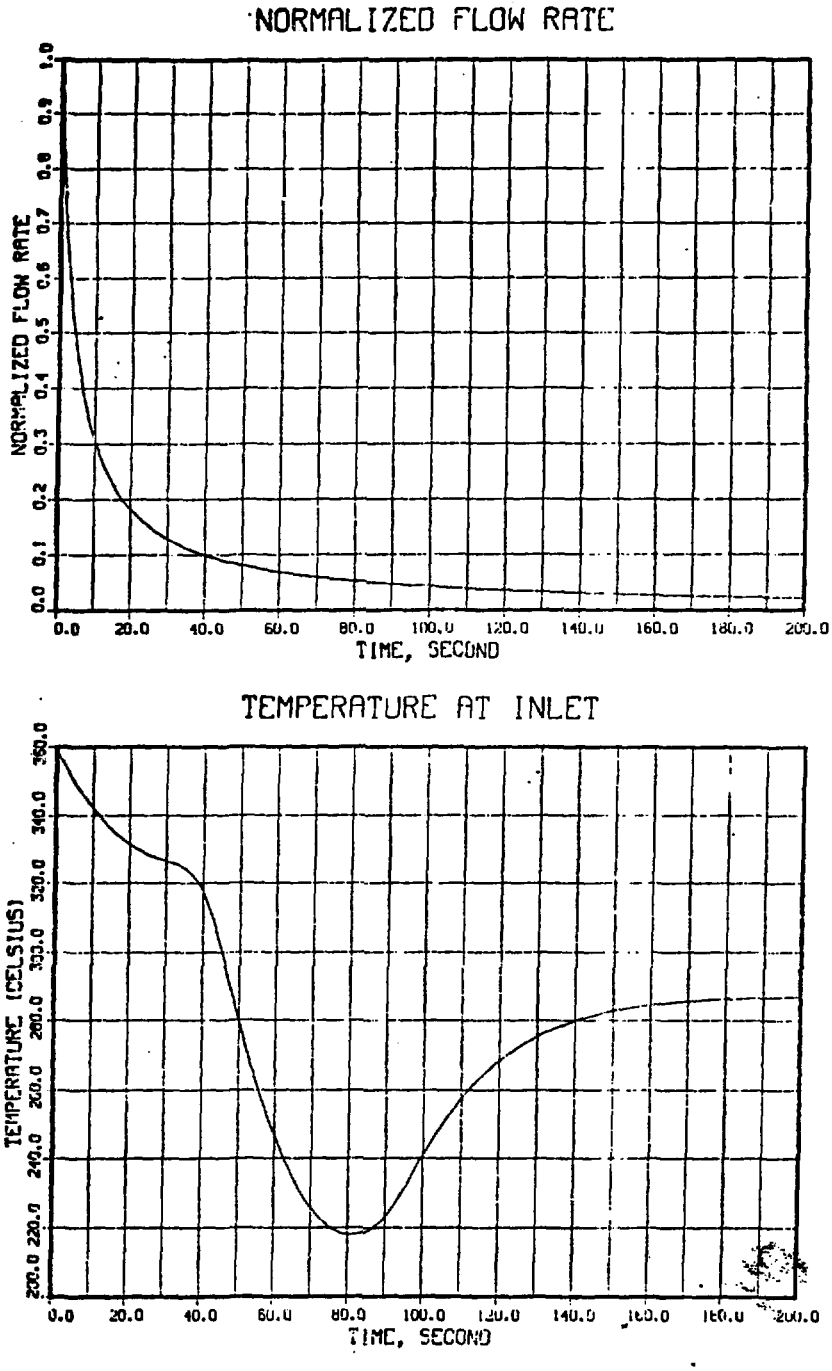

Fig. 2. **Flow and Temperature Forcing Functions at the Pipe Inlet**

ii. The temperature of the incoming sodium is uniform over the inlet cross section.

iii. Turbulent eddy transport of energy and momentum is constant throughout the transient.

iv. The pipe inner surface interacts thermally with the fluid and outer surface is adiabatic.

3.3 Numerical Results

Isothermal lines of the vertical cross section through the centerline at various times are shown in Fig. 3. This figure also shows the temperature near the wall to be warmer than at the center of the pipe due to the thermal interaction between the pipe and the relatively cooler liquid sodium.

Figure 4 shows transient liquid-sodium temperature at various axial and radial locations of the pipe. Due to the parabolic inlet-velocity distribution and the temperature decrease at the inlet, cooler sodium penetrates into the central portion of the pipe and is relatively cooler than the bottom early in the transient. As a result of the flow redistribution, a considerable top-to-bottom temperature difference is observed (about 50% of the temperature difference of the forcing function employed in the transient).

The following conclusions regarding this simulation are drawn:

i. The buoyancy effect of liquid sodium is important, and a local cold spot can be formed as a result of flow redistribution.

ii. A one-dimensional simulation of horizontal LMFBR piping is inadequate to describe the temperature and flow pattern of liquid sodium when a severe thermal-stratification condition does occur.

4. LMFBR 19-PIN ROD BUNDLE

This application of the COMMIX-1A computer code is to simulate the thermal-hydraulic behavior of a 19-rod test bundle P2, which was used in the SLSF (Sodium Loop Safety Facility) in the ETR (Engineering Test Reactor) free-convection test conducted by Argonne National Laboratory during 1976 [9].

The fuel-assembly modeling includes (1) the transient three-dimensional flow and temperature distribution of the sodium coolant; (2) the accurate representation of the volume porosity and surface permeability due to the presence of fuel rods, wire-wrap spacers, filler wires, and duct walls, and also their respective masses; (3) the transient three-dimensional temperature distributions of the fuel rods, wire-wrap spacers, filler wires, and duct walls, where axial and azimuthal conduction have been neglected in the fuel rods and the filler wires. Wire-wrap spacers and duct walls interact only with the immediately adjacent coolant; (4) an additional sweeping force has been used in the momentum equations to account for the swirl flow; and, (5) the gamma heating of the coolant, cladding, filler wires, wire-wrap spacers, and duct wall has also been accounted for.

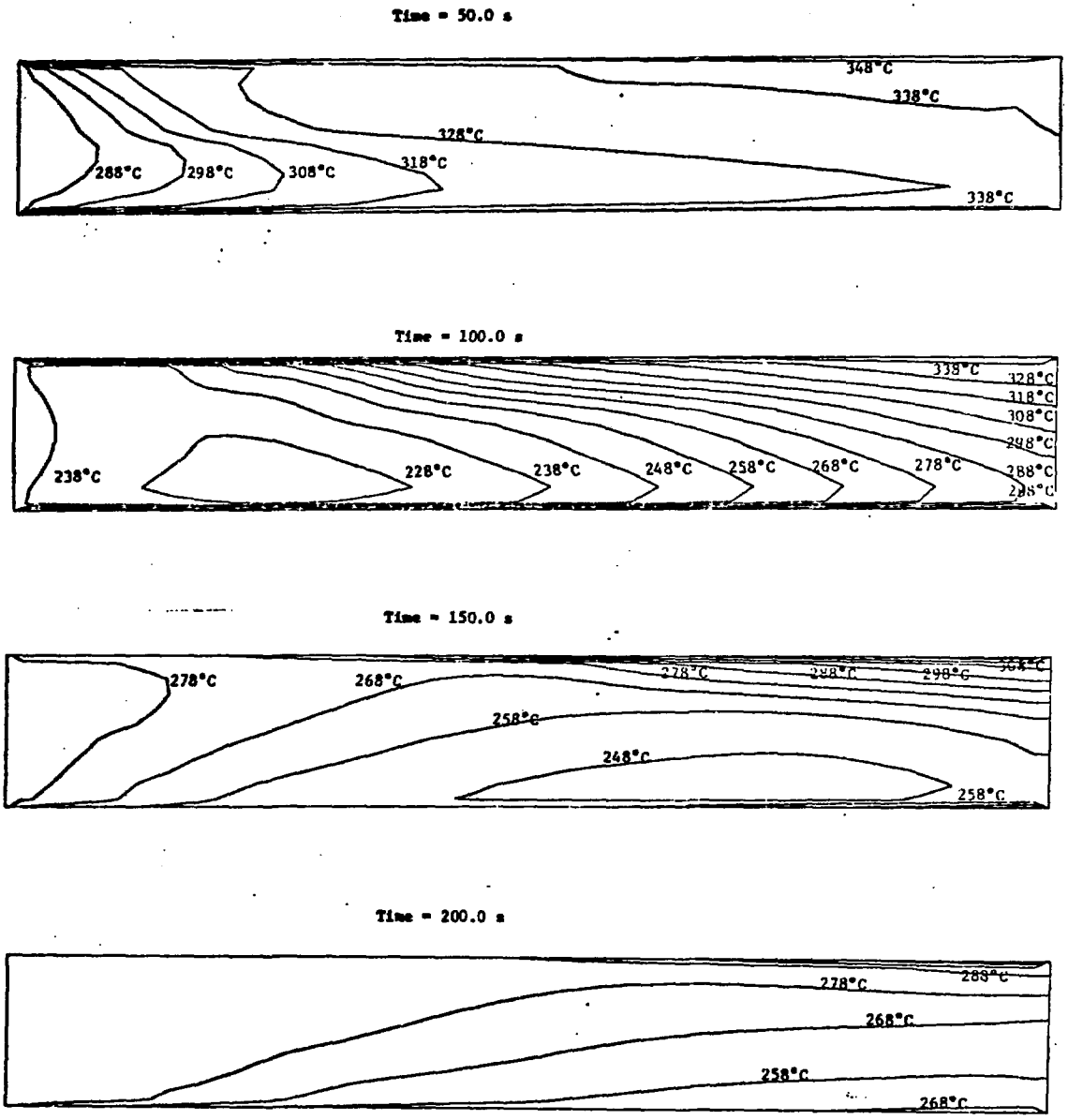

Fig. 3. Isothermal Lines of the Vertical Cross Section at Various Times

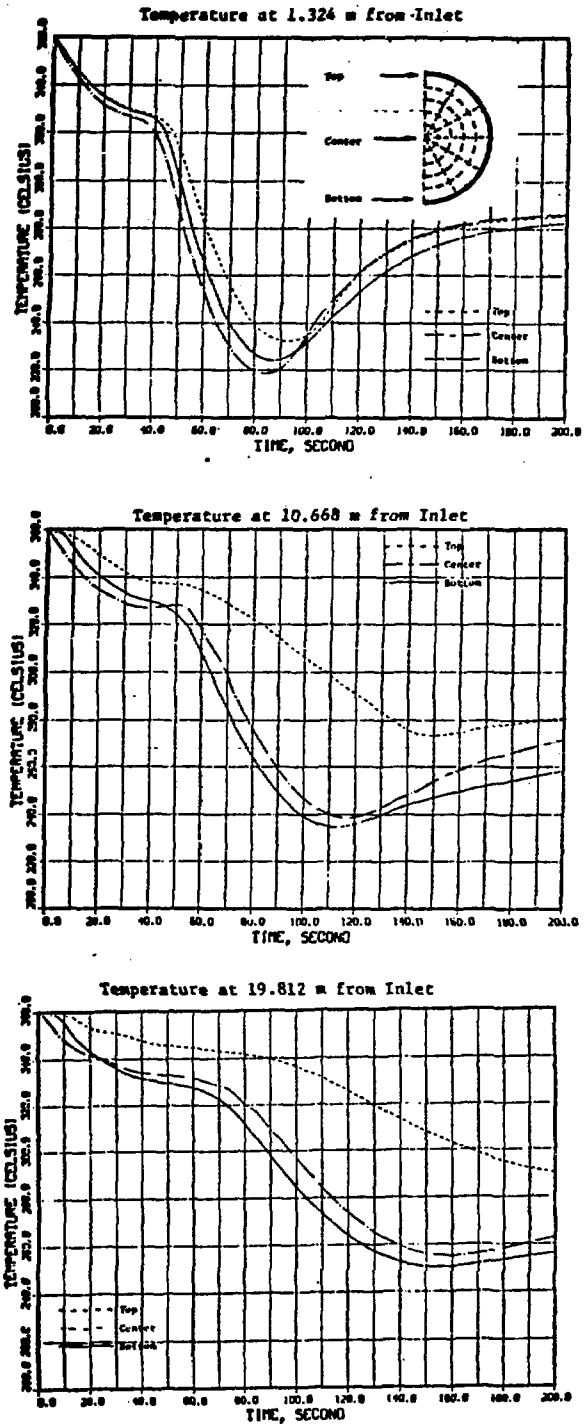

Fig. 4. Transient Liquid-Sodium Temperature at Various Radial and Axial Locations of the Pipe

4.1 Geometry

The 19 fuel rods are contained within a hexagonal duct. Each of the 19 rods has an outside diameter of 0.00584 m and is arranged in a triangular pitch of 0.00726 m. Spacing of the rods is accomplished by a wire wrapped helically around each rod. The wire spacers have a diameter of 0.00142 m when between rods, and 0.00071 m when between a rod and the duct wall. The wire is wrapped in a counterclockwise fashion (viewed looking upsream) with increasing axial level as shown in Fig. 5. The wire-wrap pitch is 0.3048 m.

The model fuel rods are composed of two materials: the fuel (UO_2, PuO_2) and cladding (316SS). The cladding occupies the annular region between (a) and (b), while the cylindrical fuel region is of radius (c), as shown in Fig. 6. The axial partitioning of the fuel rods is as shown in Fig. 7. Radially, the cladding is partitioned into two regions; the fuel is partitioned into three regions.

The rod-bundle axial length is vertically oriented. The sodium coolant enters from below and flows up through a 0.18593 m entrance region, followed by a 0.91440 m heated region, and a 0.11887 m exit region. The 1.2192 m overall length of the model fuel assembly is partitioned into 24 equal lengths, each of 0.0508 m as shown in Fig. 7. The transverse quarter-pin partitioning used in the simulation is shown in Fig. 8.

The duct walls that form the hexagonal configuration are 0.00305 m thick and are made of 316 stainless steel.

Thermocouples are located within some of the wire-wrap spacers and filler wires and also along the inner duct wall. The thermocouple positions within the model fuel assembly are shown in Figs. 7 and 8.

Uncertainties exist in the measurements: one is the exact location of thermocouples in the wire wrap under operating conditions; another is that the flow rate during the transient is below the calibrated range of the inlet EM flowmeter.

4.2 Operating Conditions

Liquid sodium enters the rod bundle uniformly with a temperature of 315°C and a velocity of 3.4 m/s. The inlet pressure is approximately 634 kPa. A total of 32574 W of heat is added to the coolant over the heated section. This heat represents both fission and gamma heating sources. The heat source in the fuel is 31271 W; the gamma heating of the cladding, wire wraps, duct walls, and coolant is about 4%, or 1303 W. The normalized axial power distribution is shown in Fig. 9, where the normalization is performed over the 0.9144 m heated length of the model fuel assembly. The normalized pin-power distribution is shown in Fig. 8, where the corner rods have a slightly higher power. The volumetric heat sources in the cladding, wire wrap, duct walls, and coolant, although different from each other, are assumed uniform over an axial level.

From the steady-state operating conditions, a flow and temperature transient occurs. The inlet velocity decreases to about 2.5% of its initial value in the first 2.5 s of the transient, as shown in Fig. 10. After leveling

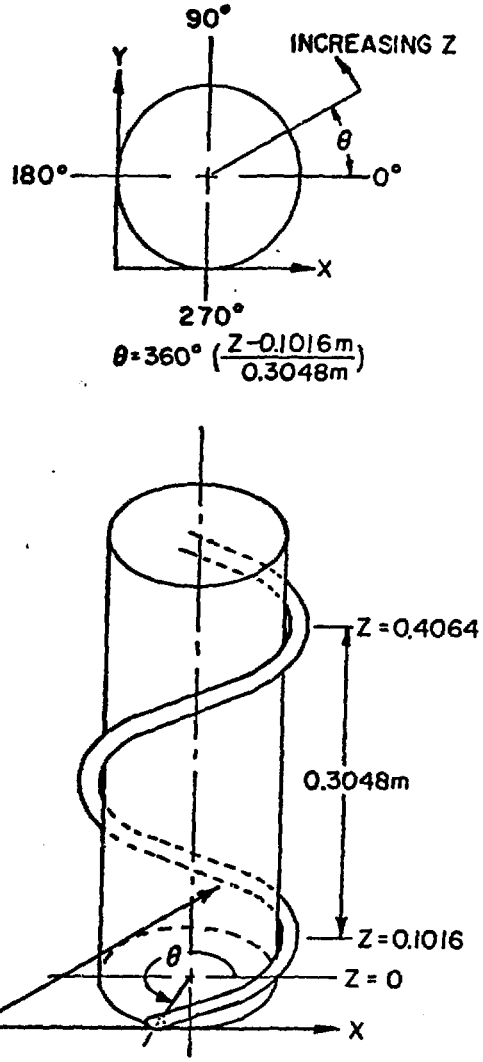

Fig. 5. Orientation and Location of Helical Wire-Wrap Spacers

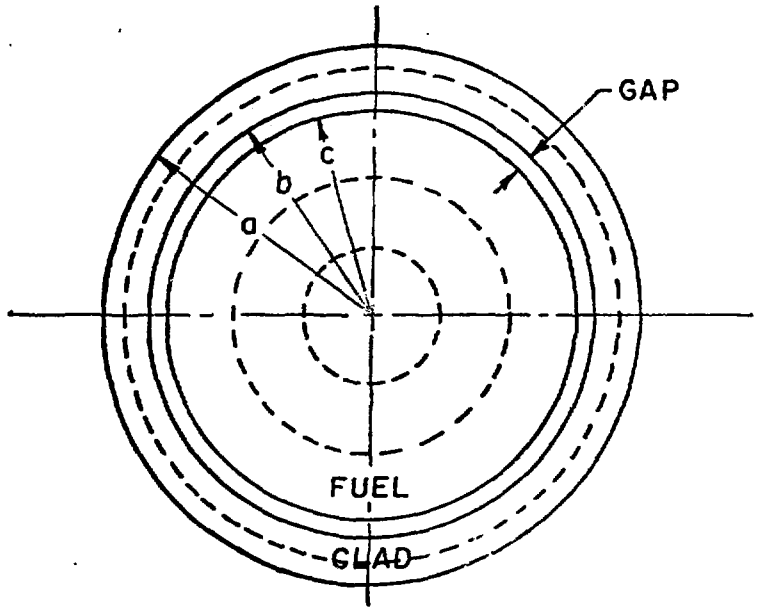

a = 0.002921 m
b = 0.00254 m
c = 0.002464 m

Fig. 6. Partitioning of Model Fuel Rods

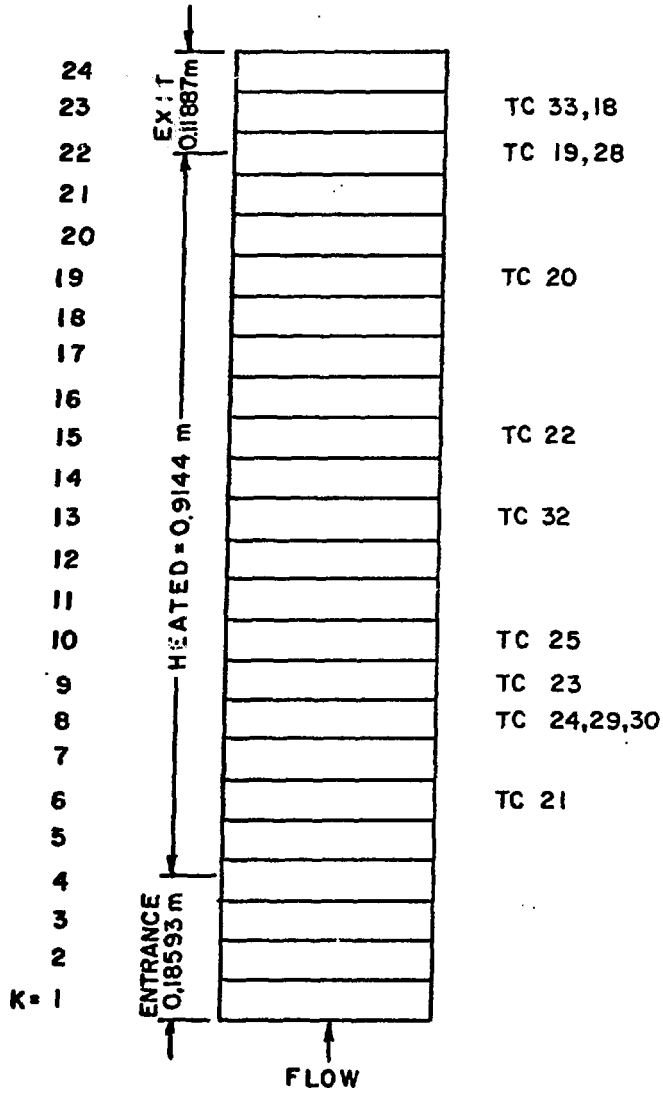

Fig. 7. AXial Partitioning of the Hodel P2 Fuel Assembly

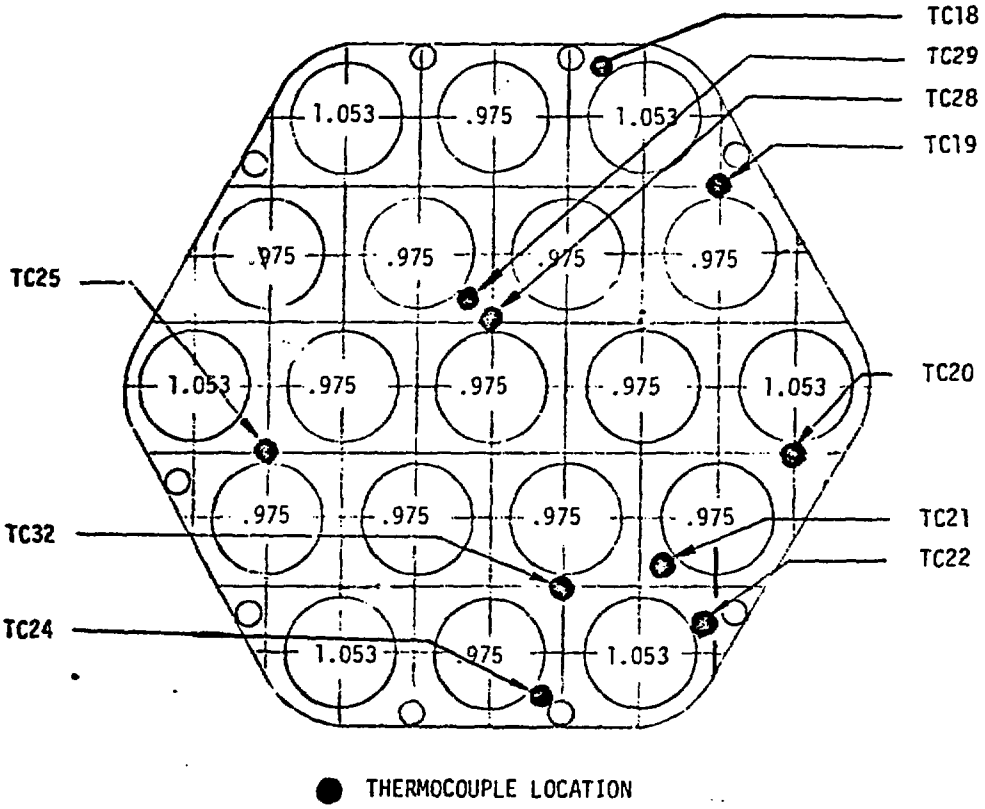

Fig. 8. Transverse Partitioning of the Model P2 Fuel Assembly

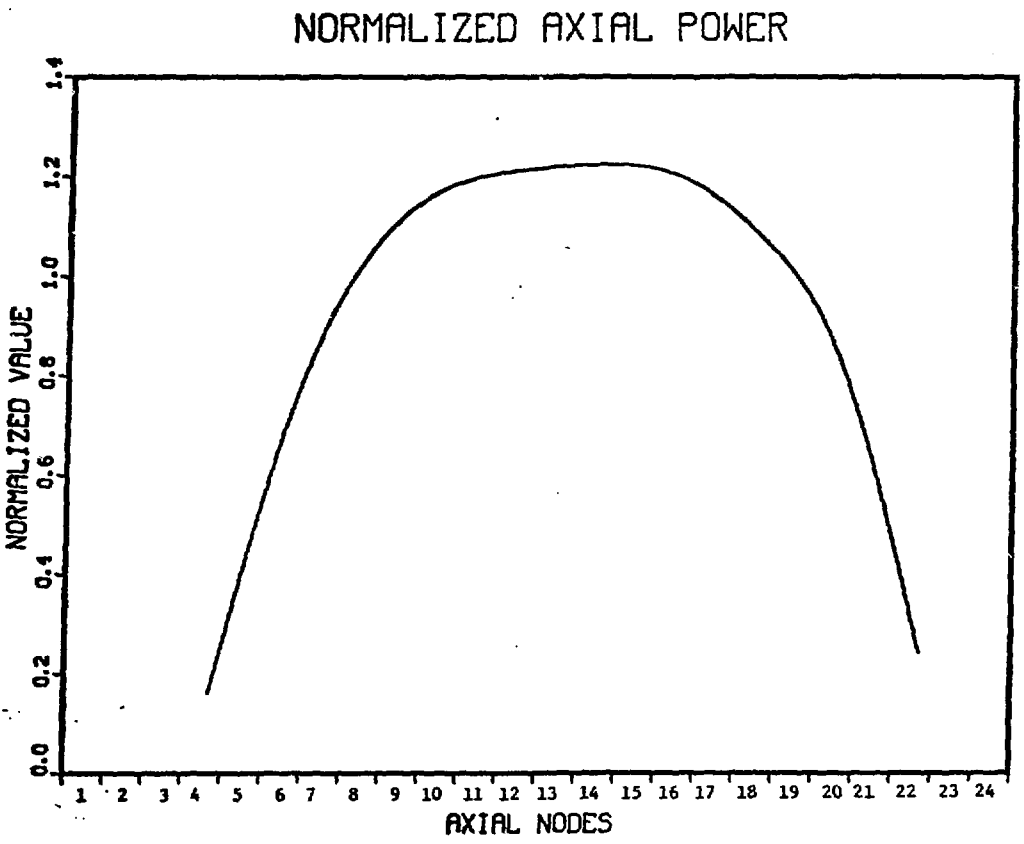

Fig. 9. Normalized Axial Power Distribution

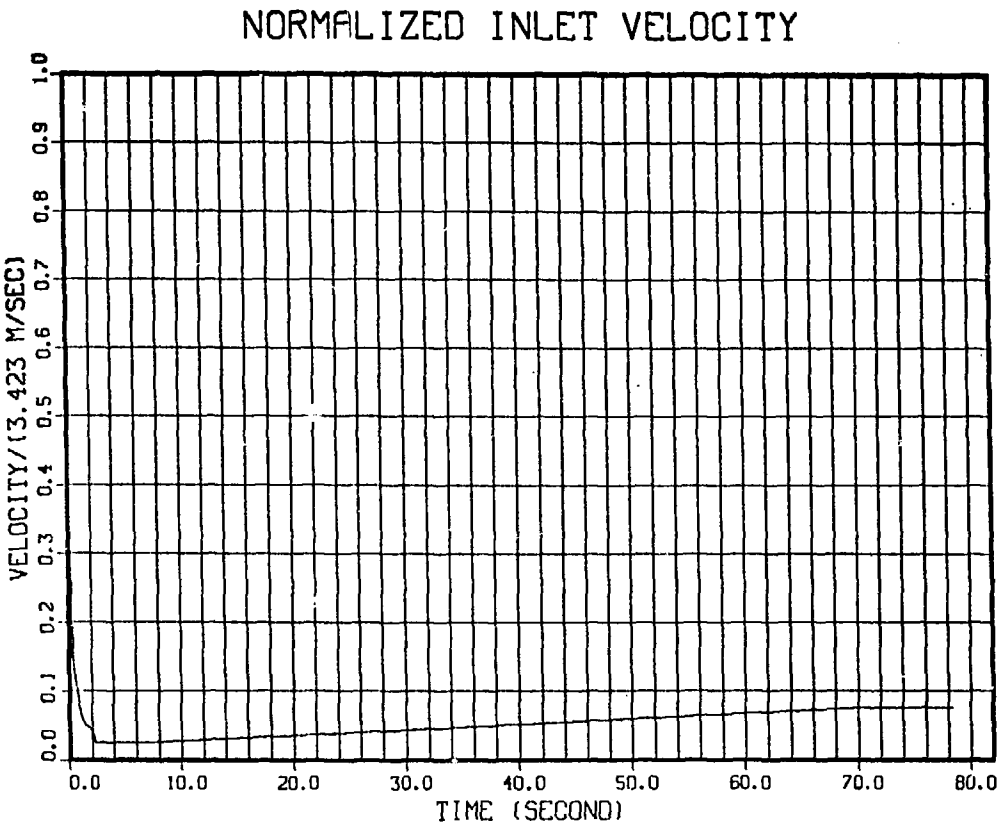

Fig. 10. Inlet Velocity Transient

off, the inlet velocity slowly increases to 7.5% of the steady-state value by 70 s, then remains constant throughout the rest of the transient.

This flow transient is the result of shutting the pumps off. The flow velocity never goes to zero, because the heated fuel assembly acts as a pump due to the bundle heating and creates a density difference, hence a pressure differential across the bundle. Throughout the entire transient the power level of the bundle remains constant.

The temperature transient is shown in Fig. 11. After being a constant 315°C for the first 7.5 s, it then slowly decreases to 295°C by 88 s, then remains at that temperature for the rest of the transient.

4.3 Numerical Results

Since the COMMIX-1A simulation gives the complete transient thermal-hydraulic field of the coolant, radial and axial temperature distributions of each fuel rod, wire wrap, filler wire, and the duct-wall temperature distributions, only a selected portion of the results are presented.

At the start of the transient, the flow velocity decreases. Due to the lower velocity, the coolant is heated for a longer time as it flows through the fuel assembly. Thus the coolant temperature begins to increase. This increased coolant temperature and decreased flow velocity reduces the amount of heat transferred from the fuel rods to the coolant; hence, the fuel rods heat up. This is particularly important toward the end of the fuel zone. As the transient proceeds, the inlet flow starts to increase and the inlet temperature starts to decrease. This action causes the sodium temperatures to peak out and decrease until they approach quasi-steady values, which are determined by the buoyancy-driven flow and decay heat. The temperature at the start of the heated section peaks first. The temperatures toward the end of the heated section peak later.

The COMMIX-1A calculation of the transient temperatures and the temperatures measured by the thermocouples located inside the wire wraps are shown in Figs. 12-14.

In this simulation of a thermal-hydraulic transient leading to a free-convection condition, the history of the inlet flow transient is the most important aspect and has the largest impact on the results, in terms of the maximum cladding temperature. The experimental data clearly show that the sodium coolant temperatures do not asymptotically approach steady state by heating up. On the contrary, they indicate an overshoot of the coolant temperatures to well above steady-state values, and a subsequent asymptotic cooling approach to steady state. These observations are correctly predicted by the COMMIX-1A code. In this transient simulation, peak coolant temperatures are below the saturation temperature and no boiling occurs. Also, flow recirculation is not observed in the bundle at anytime during the simulation.

An interesting result observed in the simulation occurs at the hot-spot location shown in Fig. 15 (K = 21). At the corner rod near the end of the heated section, the adjacent coolant temperature is hotter than the cladding temperature, indicating heat is being transferred to the fuel rod from the coolant during a portion of the transient. This is due to the axial

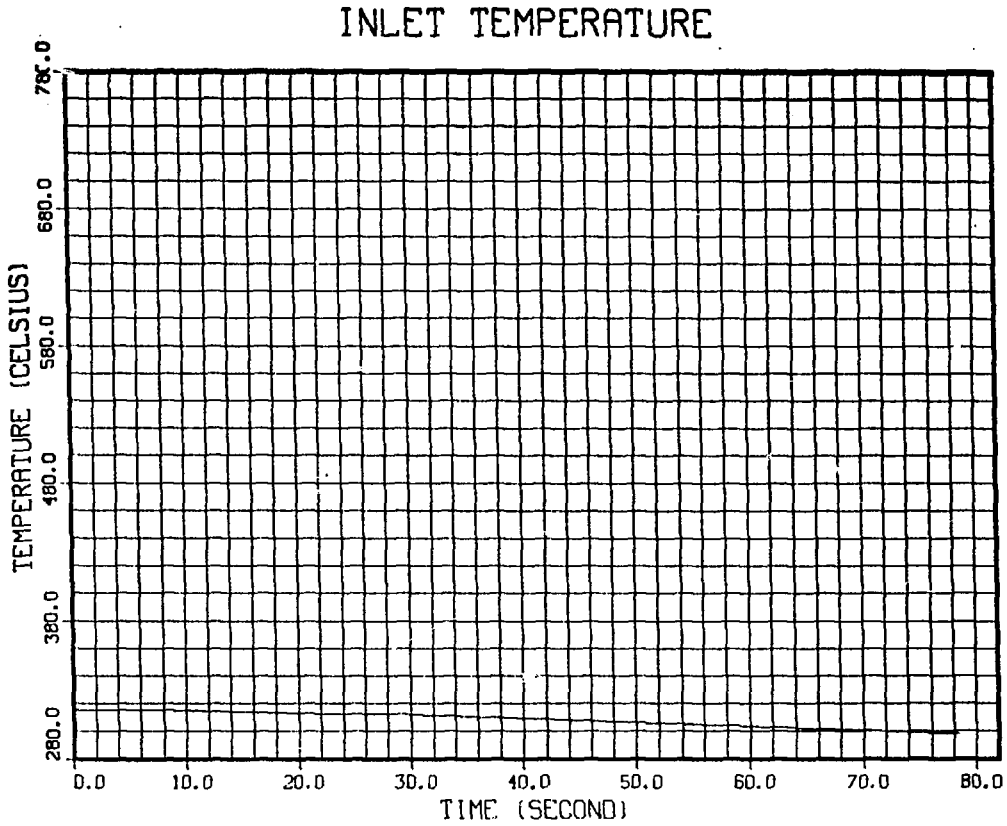

Fig. 11. Inlet Temperature Transient

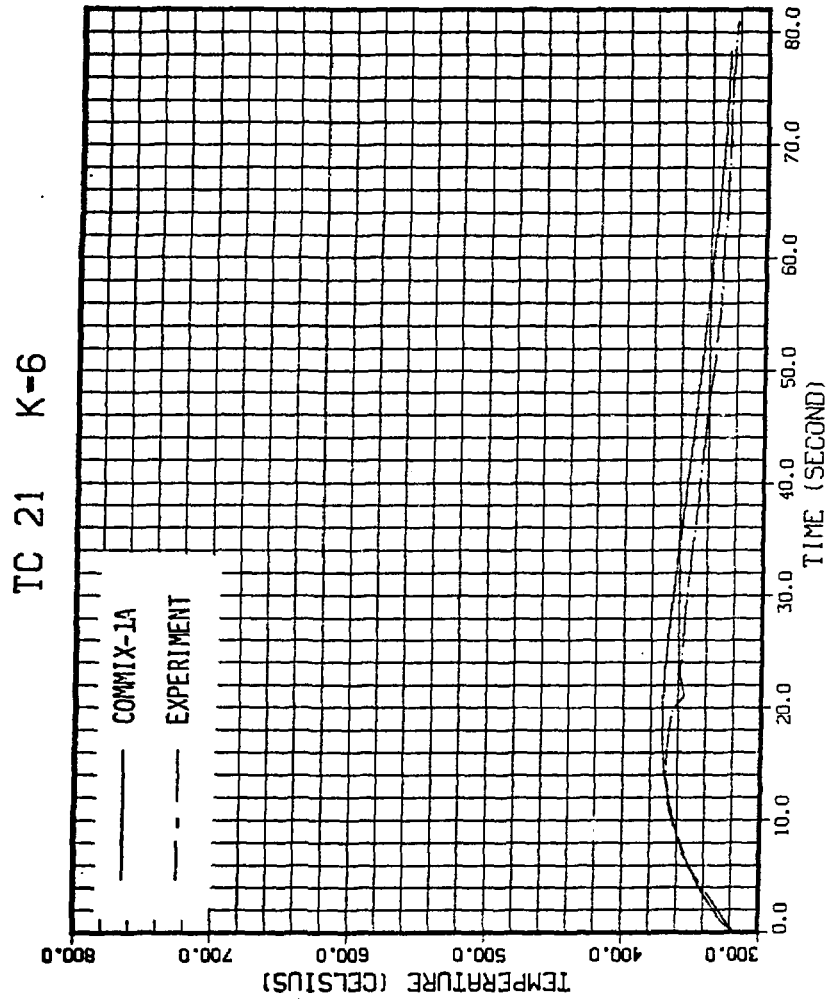

Fig. 12. Calculated Temperature Transient vs. Measurement of TC 21

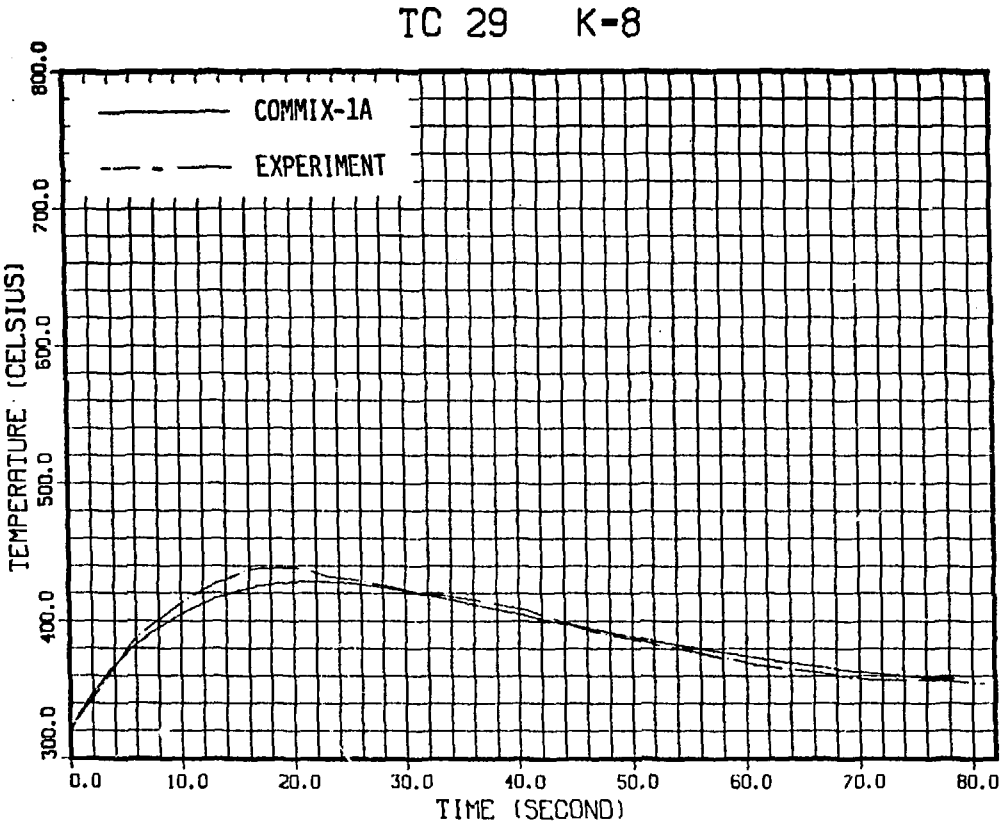

Fig. 13. Calculated Temperature Transient vs. Measurement of TC 29

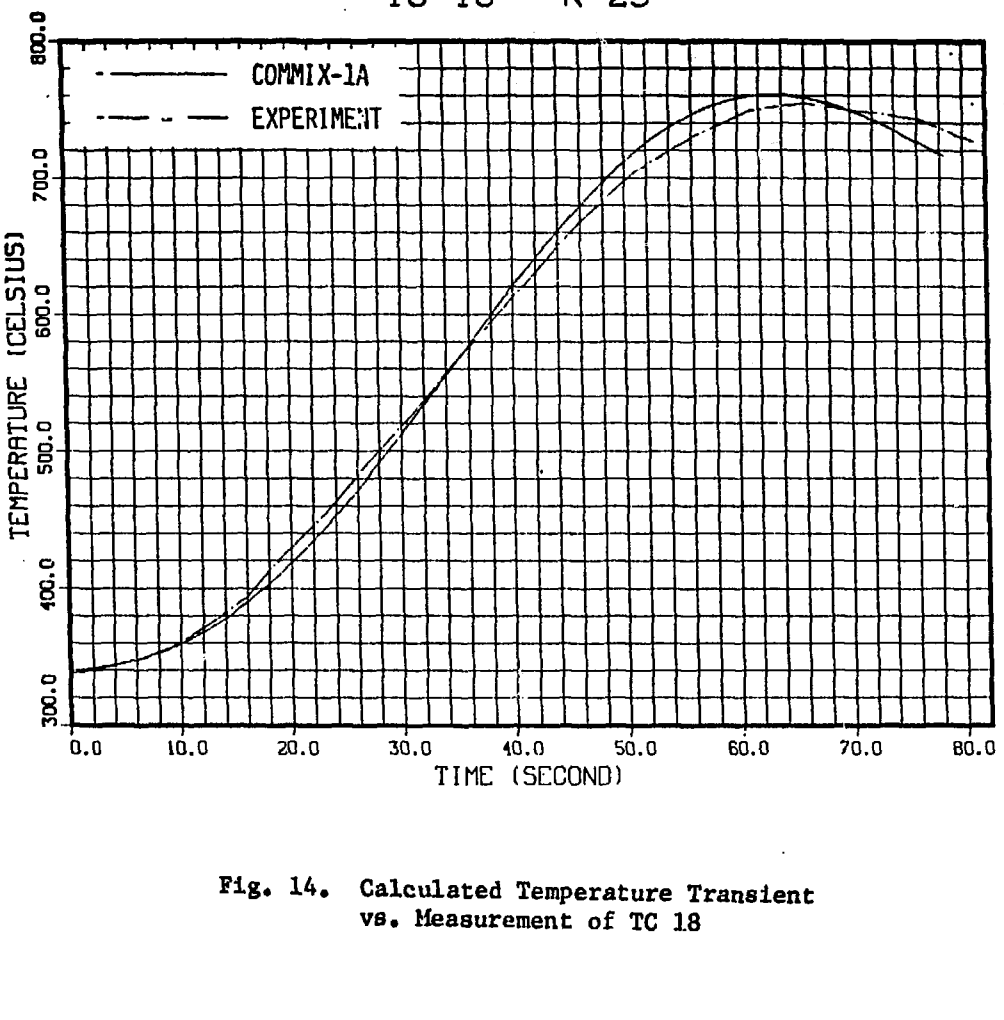

Fig. 14. Calculated Temperature Transient vs. Measurement of TC 18

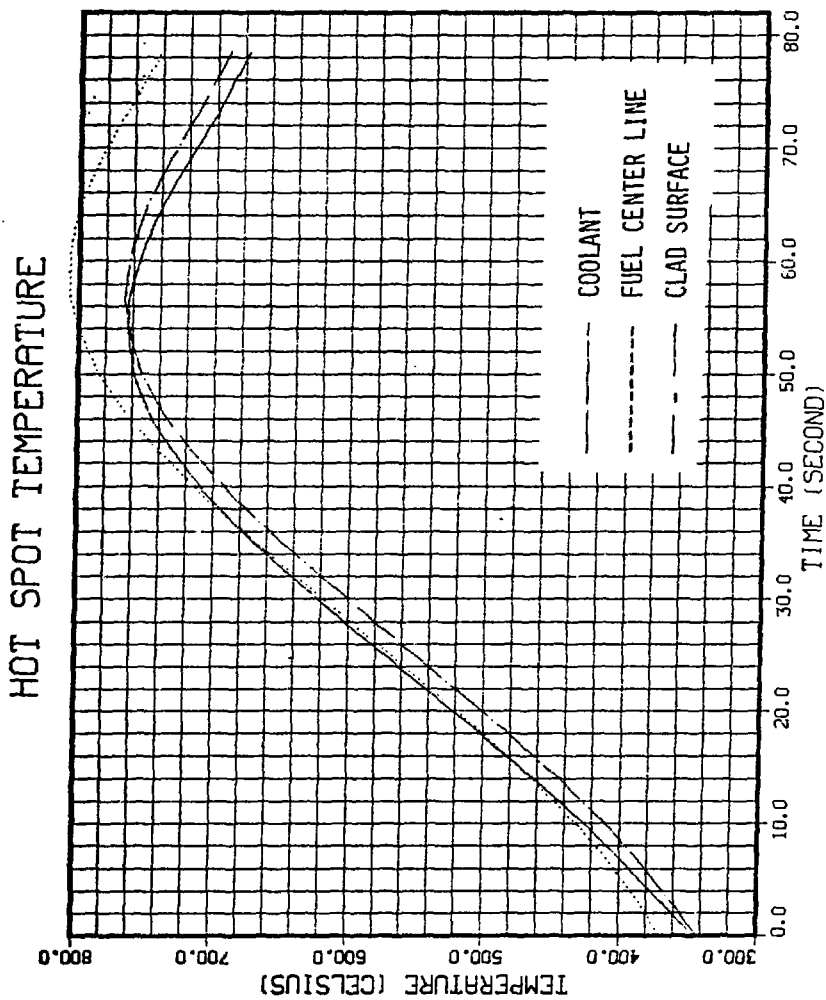

Fig. 15. Fuel, Cladding and Coolant Temperatures of Hot Fuel Rod at K = 21

power distribution where the sodium is heated a greater amount as it flows through the central portion of the heated section and transfers some heat back as it flows past the end of the heated section.

5. LMFBR OUTLET PLENUM

This simulation is of an outlet plenum undergoing both temperature and velocity reduction. The particular plenum considered was one of the experiments performed at ANL [10] on a 1/10-scale model Clinch River breeder reactor (CRBR) upper plenum with upper internal structure (UIS). The results of these water experiments have been reported [11] and run number FL19 was chosen for this simulation.

The plenum geometry is accounted for by using the quasi-continuum formulation of the conservation equations along with the volume porosity, surface permeability, and distributed resistance due to the UIS (mixing chamber, chimneys, and leakage gap).

5.1 Geometry

Flow enters the plenum from the bottom through a perforated plate containing 198 holes above the fuel assemblies and 150 holes above the blanket assemblies. The inlet above the fuel has a radius of ~0.095 m and a surface permeability of 0.37. The inlet above the blanket is a ring between r = 0.095 and 0.112 m and has a surface permeability of 0.43. Flows from the fuel and blanket regions enter the 0.06-m high mixing chamber, which contains 98 instrument posts and 19 control rods. Three exits of the mixing chamber are: 19 annular vertical chimneys above the fuel region, 10 circular vertical chimneys above the blanket region, and a 0.00254 m leakage gap around the periphery of the mixing chamber. The water flowing radially out the leakage gap is forced upward and exits into the plenum through three crescent-shaped areas. The 19 control rods extend through the 0.21 m long chimneys to the suppressor plate. Figure 16 shows the partitioning used to model the plenum in the COMMIX calculations where 60° symmetry is explicitly taken into account.

5.2 Operating Conditions

Water enters the inlet above the fuel with a velocity of 0.90 m/s and a temperature of 81.7°C, and the inlet above the blanket with a velocity of 0.18 m/s and a temperature of 49.5°C. The velocity and temperature-inlet transients which begin at 62 s are shown in Fig. 17. The inlet temperature above the blanket remains a constant 49.5°C.

5.3 Numerical Results

As the transient evolves, cold fluid is carried up to the top of the plenum until the velocity decreases and can no longer support the higher-density fluid. The flow then collapses as the cold fluid falls to the lower part of the plenum and is replaced by hot fluid coming from below. Some sloshing is detected as a hot/cold interface begins to form just above the chimney exits. As time progresses, the cold fluid leaving the chimneys spills over the UIS, fills the lower region of the plenum, and then exits. The hot/cold interface slowly moves up the plenum as heat is lost across the hot/cold interface.

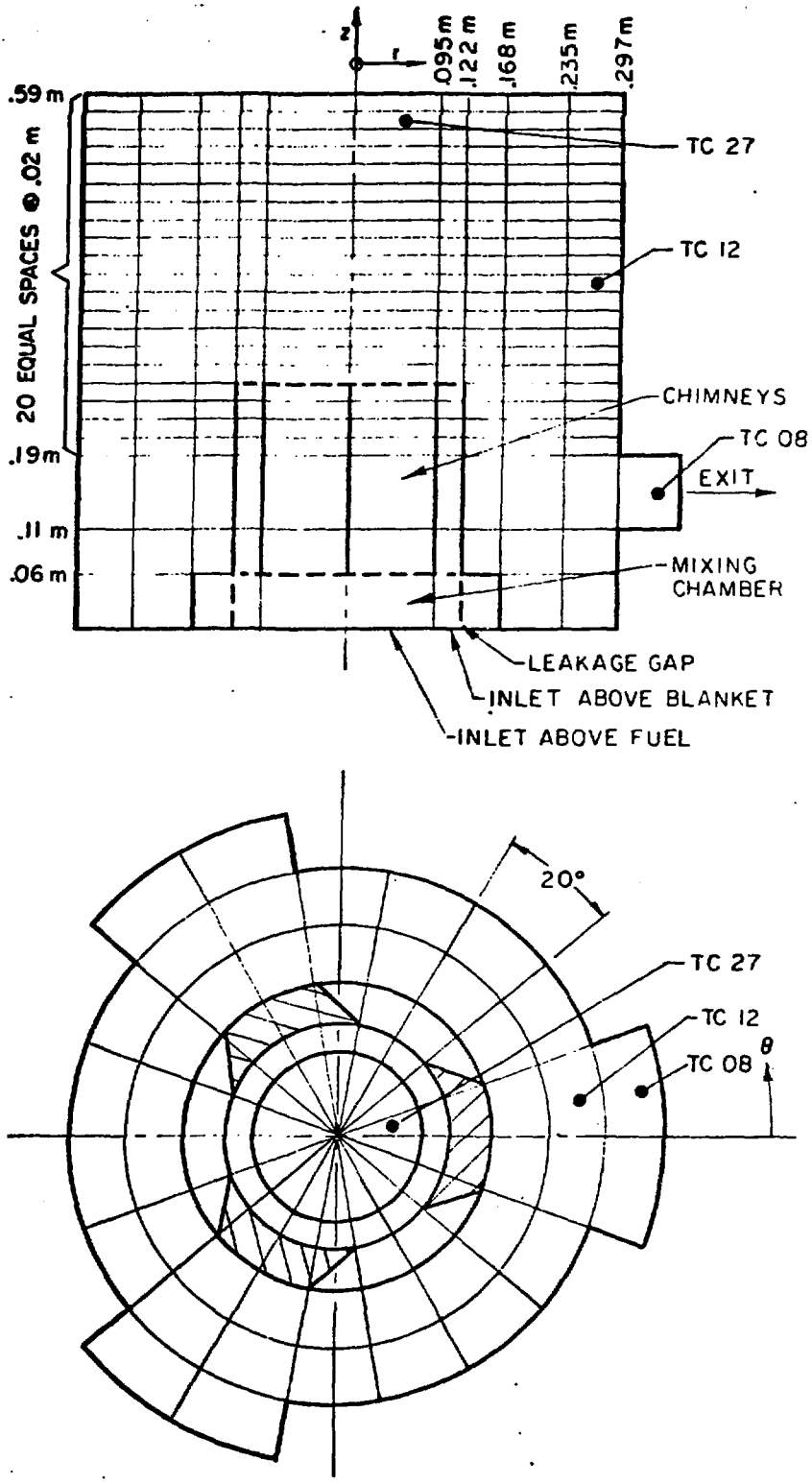

Fig. 16. Partitioning of Model CRBR Plenum

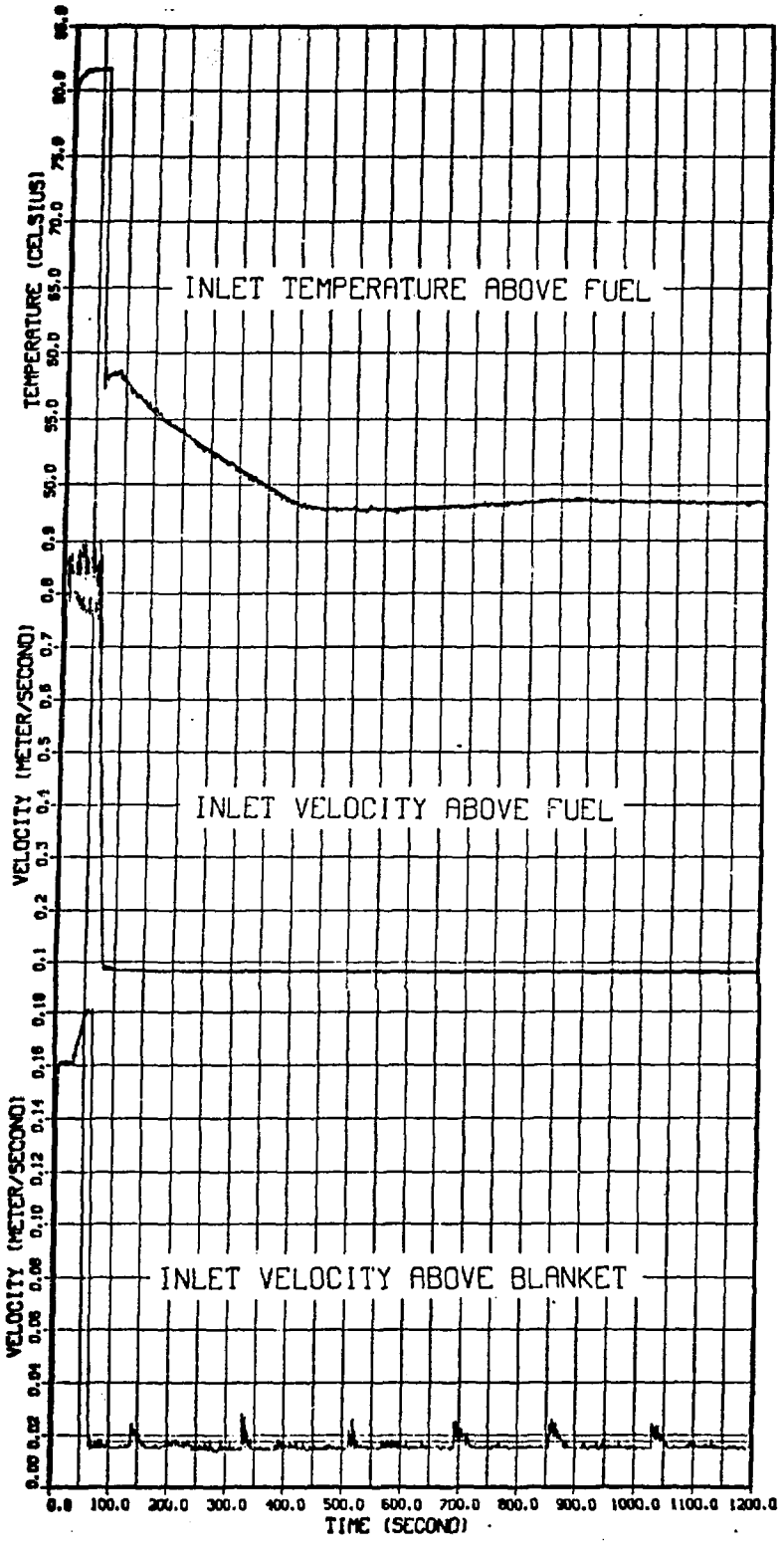

Fig. 17. Velocity and Temperature Transients

Figure 18 compares the measured and COMMIX-1A calculated results at three different locations: the temperature near the suppressor plate (TC27) above the fuel region, the temperature about midway up the plenum wall (TC12) where the hot/cold interface passes, and the exit nozzle temperature (TC08). As can be seen, agreement is quite good considering the coarseness of the mesh.

Based on the COMMIX calculations, it is concluded that:

i. Buoyancy forces are important to predict the flow pattern.

ii. Thermal interactions between the fluid and solid structures have a subtle but important effect on the thermal-hydraulic behavior under the low flow condition.

6. CONCLUSION

A new computational tool has been developed and is continually being improved to perform 3-D transient, thermal-hydraulic analyses in complex configurations. The latest version, COMMIX-1A, has been used to simulate several components where combined forced and natural convection are important. The three simulations considered here all begin with forced convection dominating. As the thermal-hydraulic transients proceed, buoyancy forces become increasingly important and change the character of the flow.

In the pipe problem, significant vertical temperature gradients can persist for some time. During these periods, a 1-D assumption can be quite misleading as to the performance. Since liquid sodium is a good conductor of heat, it is expected that fluids having a smaller thermal conductivity can have even more severe thermal gradients.

The fuel-assembly simulation revealed the importance of an accurate mass flow rate. This would indicate the need to additionally model the inlet and exit plena coupled to the fuel assembly. Simulations of this type (even the whole reactor vessel) are currently being attempted using COMMIX-1A, and results are encouraging.

The exit-plenum simulation has demonstrated some of the COMMIX-1A unique capabilities of analysis during a transient where the thermal-hydraulic character is changing dramatically. However, more code operating experience is needed to accurately track the progress of a hot/cold interface.

In these simulations, the thermal interactions between the fluid and immersed structures, as well as the containing walls, are significant and contribute noticeably to the prevailing flow character. For most practical applications in the area of combined natural and forced-convection, strong three dimensional characteristics are exhibited and normally, the region of analysis must be extended to the domain potentially having significant spatial buoyancy effects.

ACKNOWLEDGEMENTS

We want to thank Drs. R. T. Curtis and C. N. Kelber, and Mr. P. M. Wood of the United States Nuclear Regulatory Commission for their support and encouragement, and also Mrs. S. A. Moll for typing the manuscript.

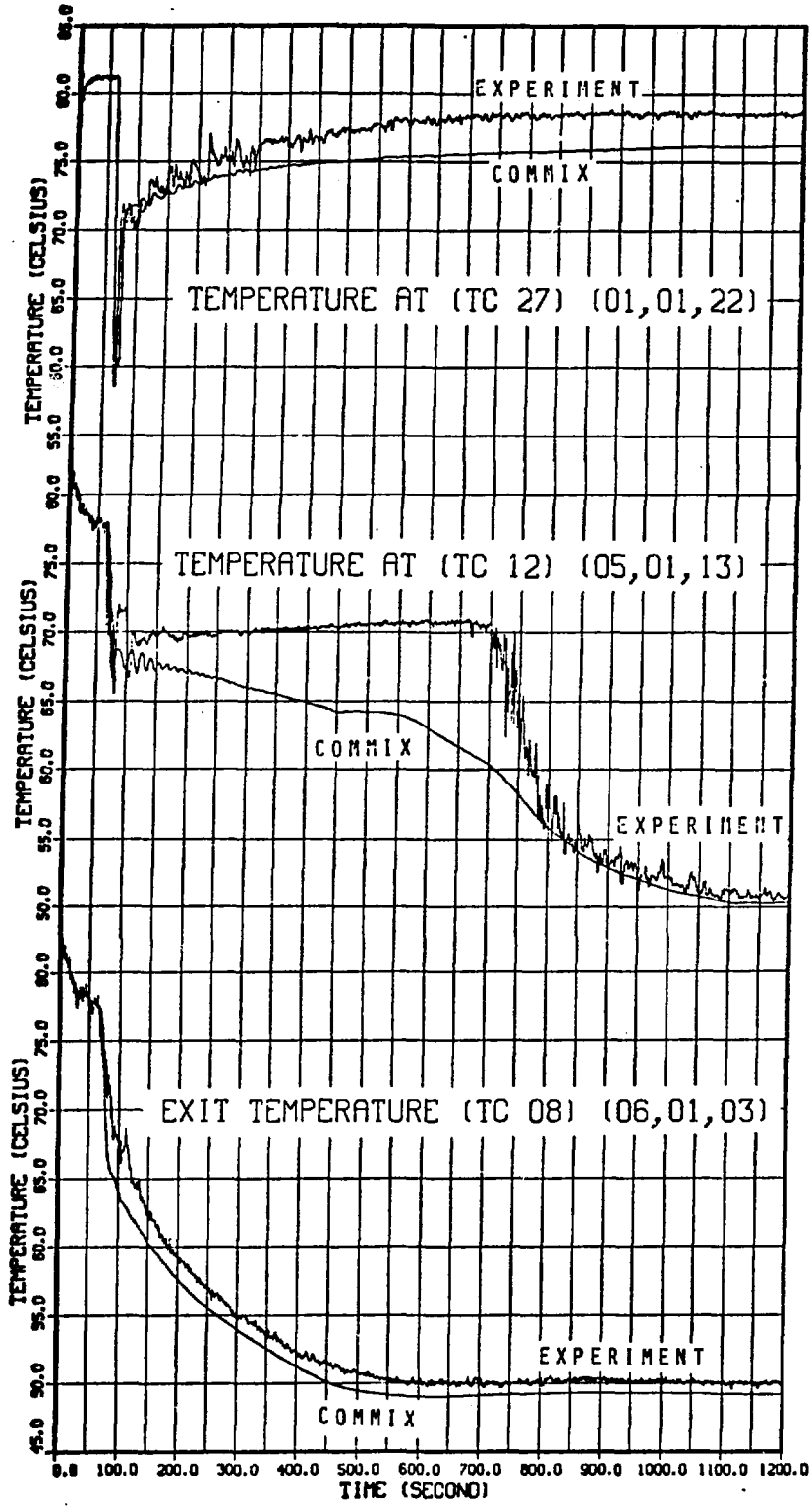

Fig. 18. Transient Temperature Comparison between COMMIX-1A Calculations and Experiment

REFERENCES

1. W. T. Sha, H. M. Domanus, R. C. Schmitt, J. J. Oras, and E. I. H. Lin, "COMMIX-1: A Three-Dimensional, Transient, Single-Phase Component Computer Program for Thermal-Hydraulic Analysis," NUREG/CR-9785, ANL-77-96 (Sept 1978).

2. H. M. Domanus, R. C. Schmitt and W. T. Sha, "Numerical Results Obtained from the Three-Dimensional Transient, Single-Phase Version of the COMMIX Computer Code," NUREG/CR-0355, ANL-CT-78-3, (Oct 1977).

3. H. M. Domanus and W. T. Sha, "Numerical Results for a Hexagonal Fuel Assembly with a Planar Blockage using the COMMIX-1A Computer Code," NUREG/CR-0483, ANL-CT-79-8 (Sept 1978).

4. H. M. Domanus, M. J. Chen and W. T. Sha, "Analysis of a Loss of Piping Integrity Transient in an LMFBR Fuel Assembly," *Trans. Am. Nucl. Soc.* 32, pp. 827-829 (June 1979).

5. H. M. Domanus, M. J. Chen and W. T. Sha, "Computational Results for a 7-Pin Hexagonal Fuel Assembly during a Flow Rundown Transient using the COMMIX-1A Computer Code," NUREG/CR-1285, ANL-CT-80-10 (Jan 1980).

6. M. J. Chen, H. M. Domanus and W. T. Sha, "Simulation of a Thermohydraulic Transient in a Pipe using the COMMIX-1A Computer Code," NUREG/CR-1323, ANL-CT-80-15 (Feb 1980).

7. W. T. Sha, H. M. Domanus, R. C. Schmitt, J. J. Oras, E. I. H. Lin and V. L. Shah, "A New Approach for Rod-Bundle Thermal-Hydraulic Analysis," Proceedings of the International Meeting on Nuclear Power Reactor Safety, Brussels, Belgium (October 16-19, 1978).

8. W. T. Sha, "An Overview of Rod Bundle Thermal Hydraulics," NUREG/CR-1825, ANL-79-10 (Nov. 1980).

9. G. L. Bordner et al, "Operation and Evaluation of the SLSF-P2 Loss-of-Flow Safety Experiments," Presented at the ASME Winter Meeting on Fluid Transient and Acoustics in the Power Industry, San Francisco, California, (Dec. 10-15, 1978).

10. J. J. Lorenz and P. A. Howard, "A Study of CRBR Outlet Plenum Thermal Oscillaton during Steady State Conditions," ANL-CT-76-36 (July 1976).

11. P. A. Howard and J. J. Lorenz, "CRBR Outlet Plenum Thermal Behavior during Transient Conditions," ANL-CT-76-49 (September 1976).

DISCLAIMER